

5.4. Ushuaia, Argentina (9/3/99– 6/20/00)

The 1999-2000 season at Ushuaia is defined as the time between the site visits 8/26/99 – 9/2/99 and 6/21/00 – 6/27/00. The season opening and closing calibrations were performed on 9/1/99 and 6/21/00 – 6/22/00, respectively. Volume 9 solar data comprises the period 9/3/99– 6/20/00. Measurements during this period were affected by several system problems. The quality of published solar data is only slightly compromised because all system malfunctions could be corrected during data processing:

- On 11/12/99, the internal irradiance standard burned out and the power supply of the lamp became defective (it is likely that the abrupt change in resistance of the lamp caused the damage to the power supply). Since it could not be repaired on site, no automatic response and absolute scans could be performed until 12/10/99, when the replacement power supply was installed. Manual monitoring of system responsivity utilizing a simple laboratory power supply suggests that the system did not change by more than 2% during the period affected. Comparisons of spectral solar measurements with measurements of ancillary sensors further confirmed that the system was stable.
- The air-conditioner of the instrument roofbox became defective on 10/13/99 and could not be repaired until the site visit in June 2000. The module was only able to heat but not to cool during this period. Temperatures inside the roofbox consequently reached values as high as 42°C during summer, which is 13°C above the set-point. During the austral winter cooling is usually not required. Between 3/15/00 and the end of the season temperatures therefore deviated by less than 4°C from the target value.

The air-conditioner is not the only temperature stabilization of the system. The most sensitive components of the system, namely monochromator and PMT, have separate temperature controls. Changes in roofbox temperature may have affected these components. The temperature of the monochromator can only be regulated by heating. Whenever the roofbox temperature was above the set-point of the monochromator temperature of 33°C, the monochromator temperature followed the roofbox temperature. In extreme cases, monochromator temperature therefore reached 42°C. As shown below, this change in temperature resulted in wavelength shifts of 0.04 nm, which is similar to typical day-to-day variation. Because of the surprisingly small effect on wavelength stability it is also unlikely that the observed temperature changes significantly affected the throughput of the monochromator.

PMT temperature is regulated with a Peltier element. Its cooling power appeared to be high enough to keep the PMT at the target temperature of -2°C for almost all days. Changes in PMT responsivity due to excessive roofbox temperature can therefore be excluded.

- The responsivity of the system in the UV-B drifted by 8% between December 1999 and the end of season. Drift-related uncertainties in solar data could be reduced to $\pm 2\%$ by application of appropriate calibration files.
- A new PMT cooler power supply was installed during the 1999 site visit. Compared to its predecessor the temperature regulation is more accurate, which is accomplished via a switching PID controller. The switching introduced, however, noise in the PMT current due to a ground loop. The problem occurred to a lesser extent also at Palmer Station (see Section 5.2), but not at the other sites. For solar elevations higher than 20° and wavelengths below 345 nm, the detection limit¹ in Volume 9 data is consequently reduced to about $0.02 \mu\text{W cm}^{-2} \text{nm}^{-1}$. This value is substantially higher than the typical value $0.001 \mu\text{W cm}^{-2} \text{nm}^{-1}$. On few occasions spikes as high as $0.2 \mu\text{W cm}^{-2} \text{nm}^{-1}$ can be found in the data set. The detection limit for solar elevations below 20° is about $0.004 \mu\text{W cm}^{-2} \text{nm}^{-1}$; the normal value is $0.0005 \mu\text{W cm}^{-2} \text{nm}^{-1}$ (see Table 2.1. in Chapter 2). The excess noise is noticeable in spectral irradiance data with wavelengths below 302 nm. We recommend not to use data with wavelengths

¹ Detection limit is defined as the standard deviation of the measured spectral irradiance at 285 nm. At this wavelength, all solar radiation is filtered out by the Earth's ozone layer. The measured value at 285 nm therefore reflects the magnitude of instrument noise, which causes the detection limit

equal to or below 298 nm. The enhanced noise also affects dose-rates calculated with Setlow's action spectrum from DNA damage. The effect on other dose-rates (e.g. "Dose3_CIE_Erythema", "Hunter", "Caldwell") is negligible, because the weighting functions of those dose-rates are centered at longer wavelengths than the "Setlow" action spectrum. At those wavelengths, spectral solar irradiance was sufficiently above the noise level. A first attempt to solve the problem was made during the site visit in 2000 by improving the ground of the PMT. This led to a marginal improvement only. The problem was finally fixed in January 2001 by adjusting the settings of the PMT cooler power supply.

- During the site visit in June 2000, the PSP and TUVR instruments installed in Ushuaia were replaced by identical instruments, which had been calibrated recently by Optronic Laboratories. The previous set of instruments was sent after the site visit to Optronic Laboratories for recalibration. The new calibration factors were applied to the data in the Volume 9 season. These factors are presumably more accurate than the old factors that were established 1988. New factors deviate by 3.9% and 10.8% for the PSP and TUVR, respectively. The direction is such that irradiance values calculated with the new factors are higher.

5.4.1. Irradiance Calibration

The irradiance standards for the 1999-2000 Ushuaia season were the lamps 200W008, M-698, and M-766. Lamp M-874 was used as traveling standard. It was calibrated by Optronic Laboratories in September 1998. Lamp 200W008 has an irradiance calibration of Optronic Laboratories from November 1996. Lamp M-698 does not have a calibration from an independent standards laboratory. For use in the 1999-2000 season, the same calibration was used as in the 1998-99 season. It was transferred to the lamp by comparing several absolute scans from M-698 and M-874, which were centered around the 1999 site visit. The method of the transfer is described in detail in Section 4.2.1.5.

Lamp M-766 has an Optronic Laboratories calibration from October 1992. Since the calibration of the lamp appears to have drifted since this time, a new calibration was established for use in the Ushuaia 1998-99 season. The same calibration was also used in the 1999-2000 season. The calibration was transferred from M-874 in the same way as for M-698. For M-874, the Optronic Laboratories calibration values from 1998 have been used, and absolute scans applied from days 8/24/99 and 8/26/99.

Figure 5.4.1 shows a comparison of all lamps at the beginning of the season (9/1/99). All lamps agree to within $\pm 1\%$. The good agreement of lamps M-698 and M-766 with M-874 can be expected as both lamps were calibrated with M-874 at approximately the same time. The validity of the calibration of M-874 is confirmed by the good agreement with lamp 200W008, which has an independent calibration.

Figure 5.4.2 shows the comparison of all site standards with M-874 at the end of the season. Lamps M-698 and M-766 agree to within $\pm 1\%$. The difference between M-874 and 200W008 is similar in the UV but slightly larger in the visible. The standards 200W008, M-698, and M-766 were measured several times back-to-back during the season. The pattern of the observed differences is very similar to the pattern found in the season closing calibrations.

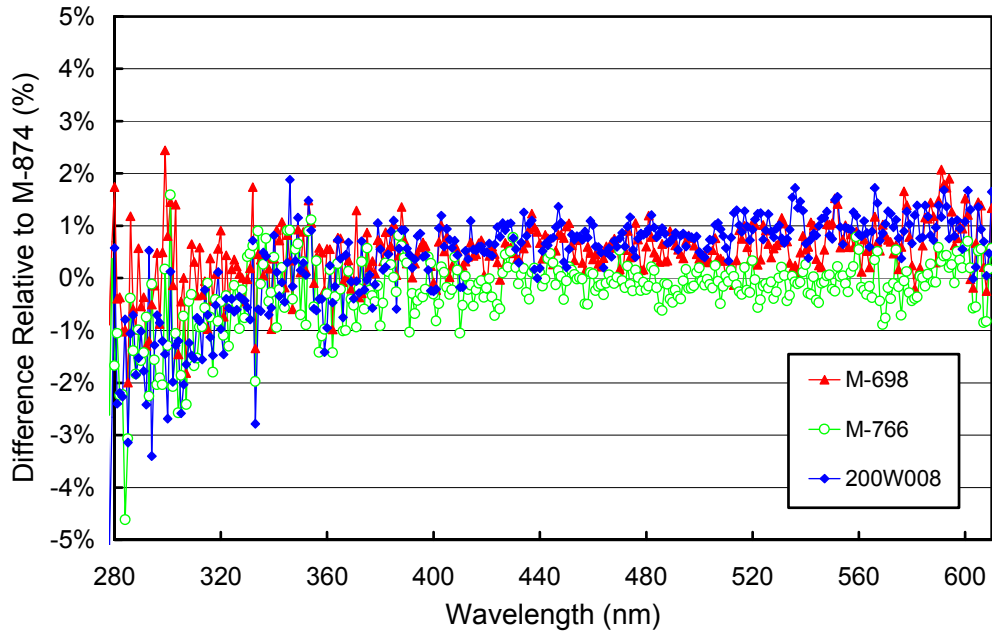


Figure 5.4.1. Comparison of Ushuaia lamps M-698, and M-766, and 200W008 with the BSI traveling standard M-874 at the beginning of the season (9/1/99).

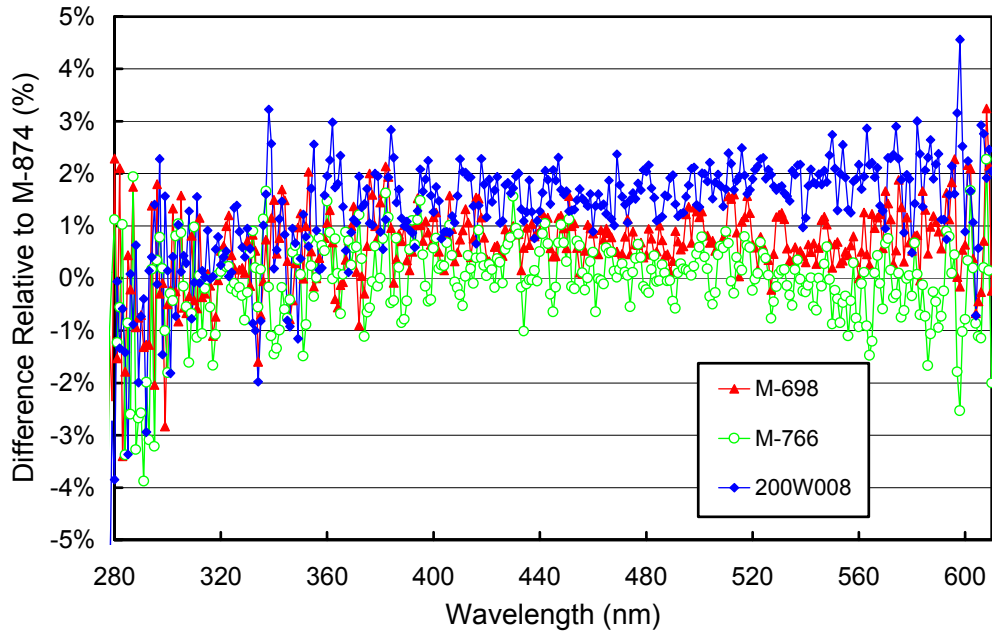


Figure 5.4.2. Comparison of Ushuaia lamps M-698, and M-766, and 200W008 with the BSI traveling standard M-874 at the end of the season (6/21/00 – 6/22/00).

5.4.2. Instrument Stability

The stability of the spectroradiometer over time is primarily monitored with bi-weekly calibrations utilizing site irradiance standards and daily response scans of the internal irradiance reference. The stability of the internal lamp is monitored with the TSI sensor, which is independent from possible monochromator and PMT drifts.

By logging the PMT currents at several wavelengths during response scans, changes in instrument responsivity can be detected. Figure 5.4.3 shows the changes in TSI readings and PMT currents at 300 and 400 nm, derived from the daily response scans between the season start and 12/9/99, the day when the power supply was replaced. Because of the defect of the power supply no automatic response scans were performed during 11/12/99 and 12/10/99, explaining the gap in Figure 5.4.3. Until 11/11/99, TSI measurements were stable to within $\pm 1\%$, indicating the good stability of the internal irradiance reference lamp. In the same period, PMT currents drifted downward by approximately 5%. Calibrations with the 200-Watt site standards performed in the same period showed a similar drift. Based on these results, the period between the season start and 12/9/99 was broken in three sub-periods, denoted Period 1-3 in Figure 5.4.3. The irradiance assigned to the internal lamp was calculated separately for each of the periods. From all calibrations in a specific period, irradiance spectra for the internal lamp were calculated and the irradiance spectrum assigned to the lamp is the average of the individual spectra (see Section 4.2.1.2 for details). Figure 5.4.4 shows the ratio of the spectral irradiance values applied in Periods 2 and 3, to the spectral irradiance of Period 1. There is a change of up to 3% in the mean irradiance assigned to the internal lamp.²

As mentioned above, not only the power supply but also the internal irradiance lamp broke on 11/12/99. The lamp was replaced on 11/13/99. Between 11/17/99 and 12/08/99 seven response scans were manually conducted with this lamp, using a laboratory power supply with no computer interface. Since no absolute scans were performed during this period no irradiance values could be assigned to the new reference lamp. The measurements were therefore used to monitor system stability only.

Data scans performed in the problematic period between 11/12/99 and 12/10/99 were “paired” with the last good response scan of Period 3 measured on 11/11/99. Thus, the system was “let to believe” that power supply and response lamp are still functional. This method is only appropriate if the system responsivity during the affected period is stable. The analysis of the manually performed response scans indicates that this is the case; all scans agreed to within $\pm 1\%$ (see also Figure 5.4.6). To further verify that the system was stable in the problematic period, TSI-measurements performed during solar scans were compared to spectral solar measurements that have been weighted with the TSI responsivity-function. Figure 5.4.5 demonstrates that this ratio shows no significant change between 10/15/99 and 12/31/99. This period includes a one-month period before the power supply break, the period when only the spare power supply was available, and a three-week period after the new power supply was installed.

Figure 5.4.6 shows the changes in TSI readings and PMT currents at 300 and 400 nm, for the remainder of the season (12/10/99-6/20/00). During this period TSI measurements were stable to within $\pm 1\%$, indicating that also the new internal lamp was stable. PMT-currents at 300 and 400 nm drifted by 2-4%, similarly as during the first part of the season. Calibrations with the 200-Watt site standards performed between 12/10/99-6/20/00 suggested that also the second part of the season has to be divided in four sub-periods, denoted Periods 4 – 7. Figure 5.4.7 shows the ratio of the spectral irradiance measured in Periods 5 – 7, to the spectral irradiance of Period 4. There is a change of approximately 2% from period to period, which is

² Note that this change does not mean that the lamp actually became brighter, as the TSI measurements of the lamp (Figure 5.4.3) are stable. More likely, there was a change in the upper part of the collector and/or the optics block which caused the internal lamp to appear brighter relative to external 200-Watt calibration lamps. By assigning different calibrations to internal lamp in Periods 1-3, possible changes in the optics block were corrected. During the 1998-99 season similar changes were observed. They were likely caused by dust from wear of the shutter, which collected on the relay lens. During the site visit in 2000, no dust was found and all other parts of the optics appeared to be clean. The actual reason of the observed drift is therefore unknown.

probably caused by changes in the optics block (see footnote on previous page). By assigning different calibrations to the internal lamp in Periods 4-7, these changes in instrument responsivity were corrected.

As explained above, the irradiance assigned to the internal lamp in each period is the average of individual spectra sampled in that period. The standard deviation of the individual spectra allows estimating the variability of the calibrations in each given period. Figure 5.4.8 shows that the standard deviation is less than 1.5% of the average for all periods, except for Period 4. Period 4 is the first period after installation of the new power supply on 12/10/99. There are only four absolute scans contributing to this period, three from 12/13/99 and one from 1/3/00. The three scans from 12/13/99 are not as consistent as shown in Figures 5.4.1 and 5.4.2, for unknown reasons. There is therefore a higher calibration uncertainty for Period 4.

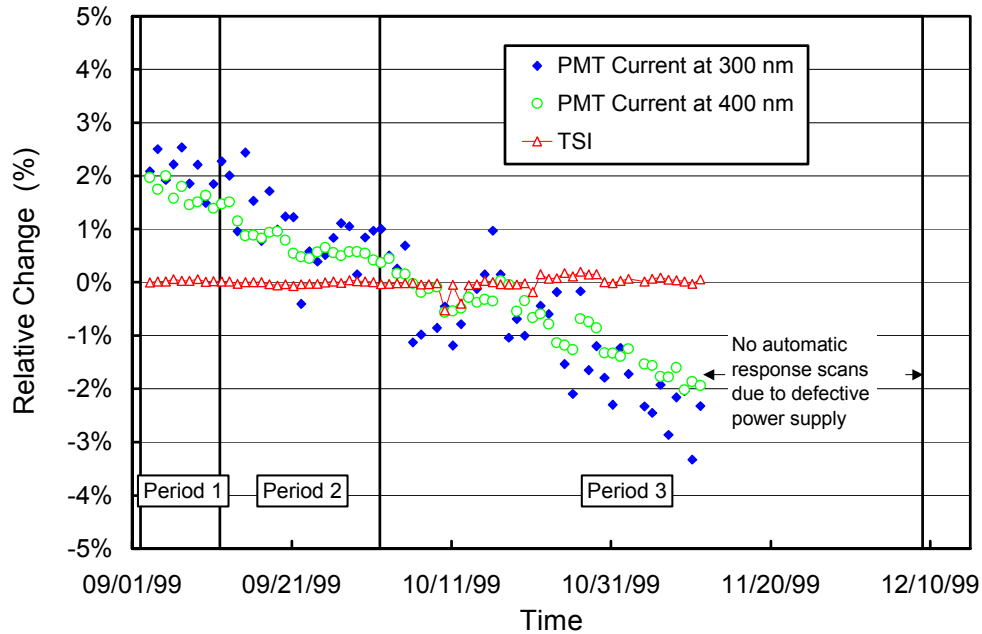


Figure 5.4.3. Time-series of PMT current at 300 and 400 nm and TSI signal during measurements of the response lamp during the Ushuaia 1999-2000 season, Period 1-3. The data is normalized to the average of all three periods.

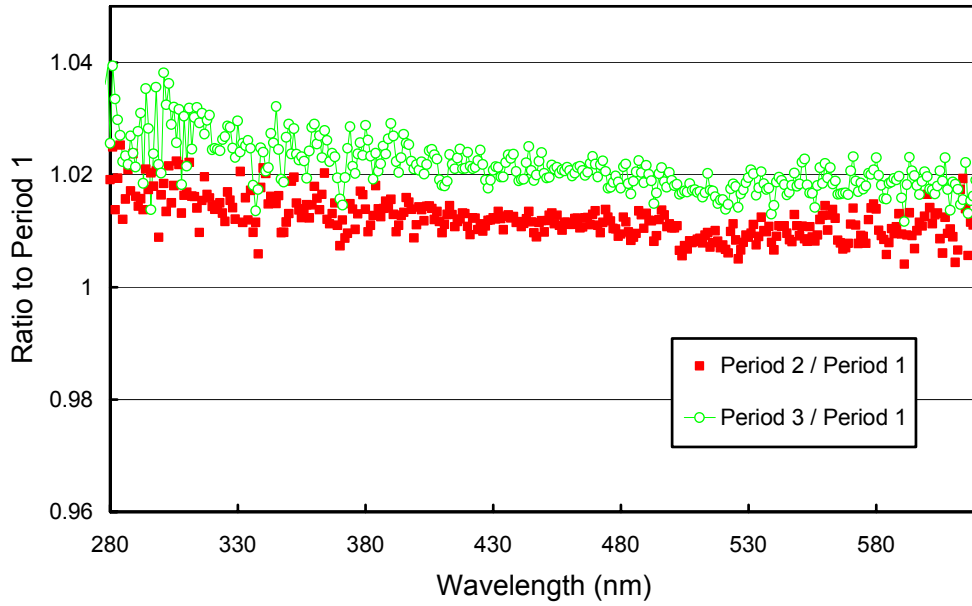


Figure 5.4.4. Ratios of irradiance assigned to the internal reference lamp in Period 2 and 3, reference to the irradiance of Period 1.

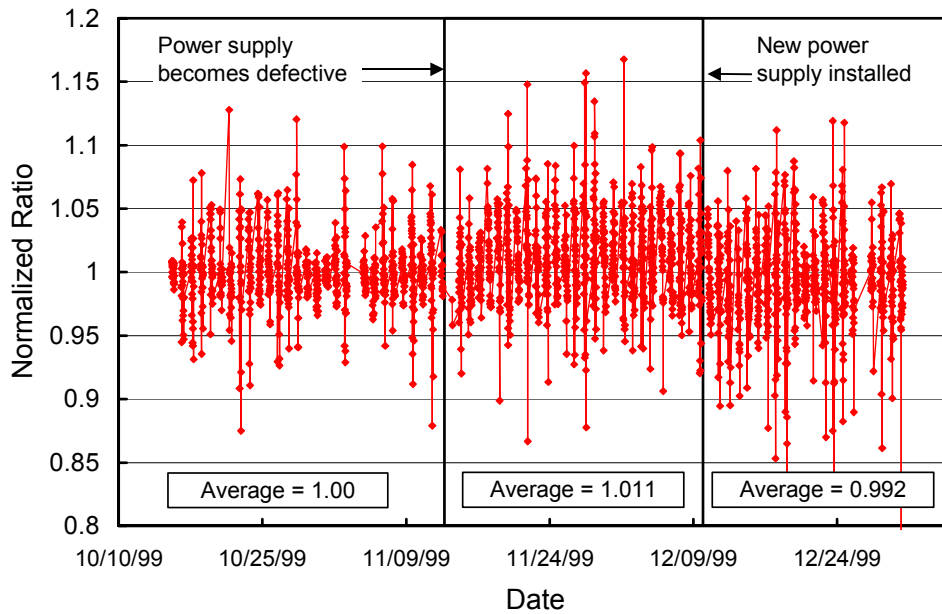


Figure 5.4.5. Ratio of TSI measurements during solar scans and spectral solar measurements that were weighted with the response function of the TSI. Only measurements with solar zenith angles smaller than 60° were evaluated. The ratio is normalized to the measurements during the period immediately before the power supply became defective.

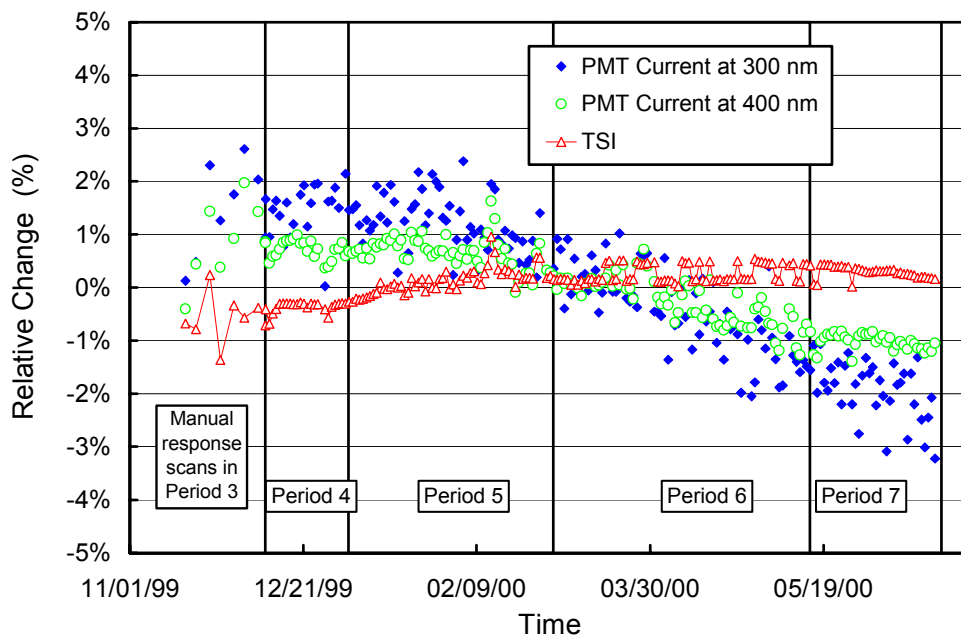


Figure 5.4.6. Time-series of PMT current at 300 and 400 nm and TSI signal during measurements of the response lamp during the Ushuaia 1999-2000 season, Period 4-7. The data is normalized to the average of all four periods. Data points before start of Period 4 are based on manually performed response scans with a simple laboratory power supply.

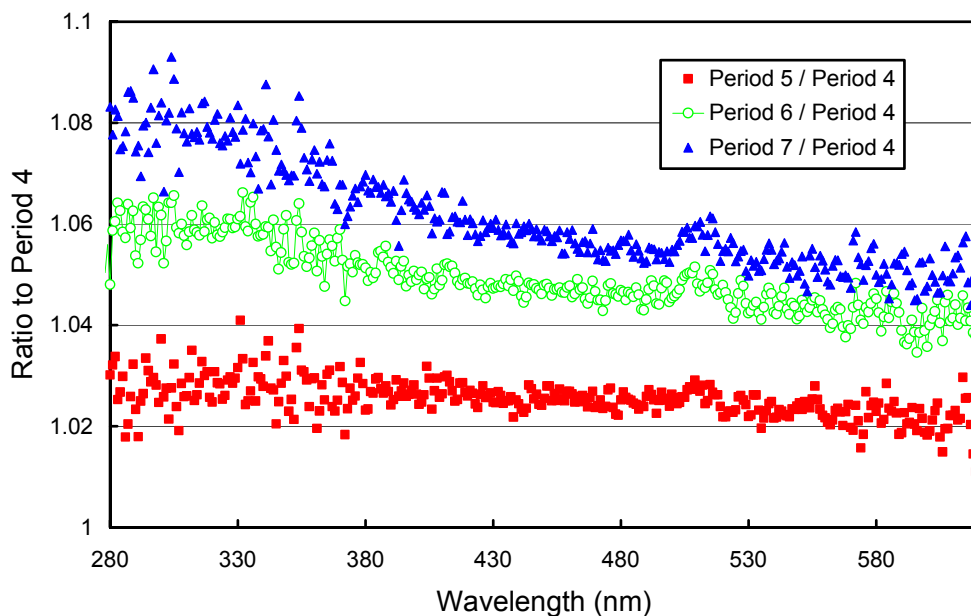


Figure 5.4.7. Ratios of irradiance assigned to the internal reference lamp in Periods 5 – 7, referenced to the irradiance of Period 4.

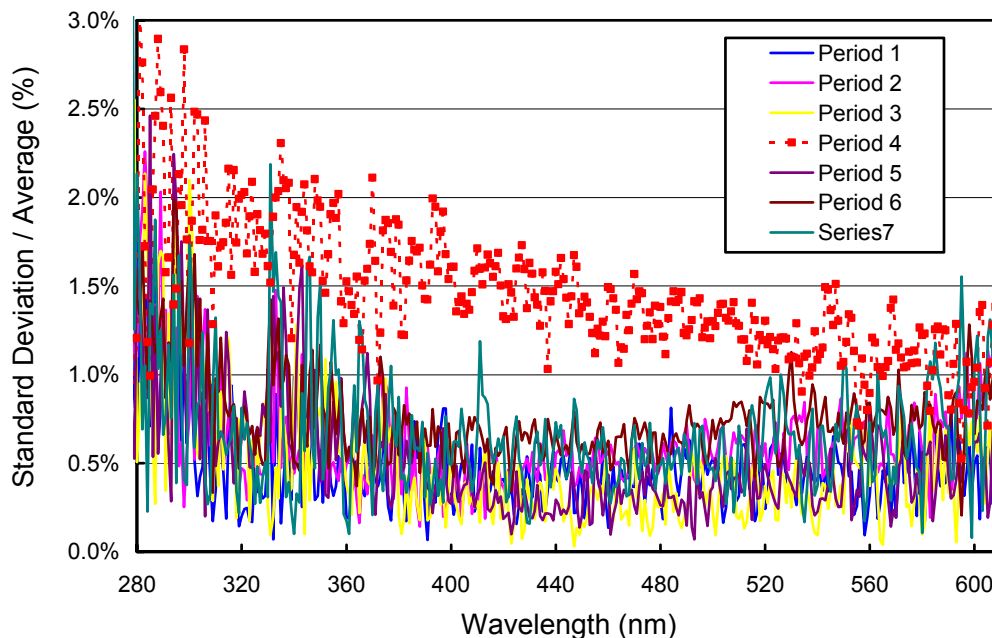


Figure 5.4.8. Ratio of standard deviation and average calculated from the absolute calibration scans measured during the Ushuaia 1999-2000 season. The ratio is calculated separately for each of the seven periods.

5.4.3. Wavelength Calibration

Wavelength stability of the system was monitored with the internal mercury lamp. Figure 5.4.9 shows the differences in the wavelength offset of the 296.73 nm mercury line between two consecutive wavelength scans. In total, 313 scans were evaluated. For 91% of the scans is the difference in the wavelength offset to neighboring scans less than ± 0.035 nm. Changes larger than ± 0.1 nm occurred for 11 scans (3.5%) only. Nine of those scans were performed on 11/12/99 when the power supply became defective. Data scans from the affected period were excluded from the analysis.

After the data was corrected for day-to-day wavelength fluctuations, the wavelength-dependent bias between this homogenized data set and the correct wavelength scale was determined with the Fraunhofer-correlation method, as described in Chapter 4. The thick lines in Figure 5.4.10 shows the correction function. In order to demonstrate the difference between the result of the Fraunhofer-correlation method and the method that was historically applied, Figure 5.4.10 also includes a correction function that was calculated with the “old” method, i.e., the function is based on internal wavelength scans only. There is a difference of about 0.16 nm between both functions. Compared to other sites, this is comparatively large but the comparison between internal and external wavelength scans (see below) shows that this difference is real.

After the data was wavelength corrected using the shift function described above, the wavelength accuracy was tested again with the Fraunhofer method. The results for noon-time spectra are shown in Figure 5.4.11 for four UV wavelengths. Residual shifts are generally smaller than ± 0.05 nm and only few days show shifts greater than ± 0.1 nm. Mostly affected is the 310 nm dataset due to lower signal levels, which reduce the precision of the correlation method. The actual wavelength uncertainty may be a little larger due to possible systematic errors of the Fraunhofer-correlation method (see Section 4.2.2).

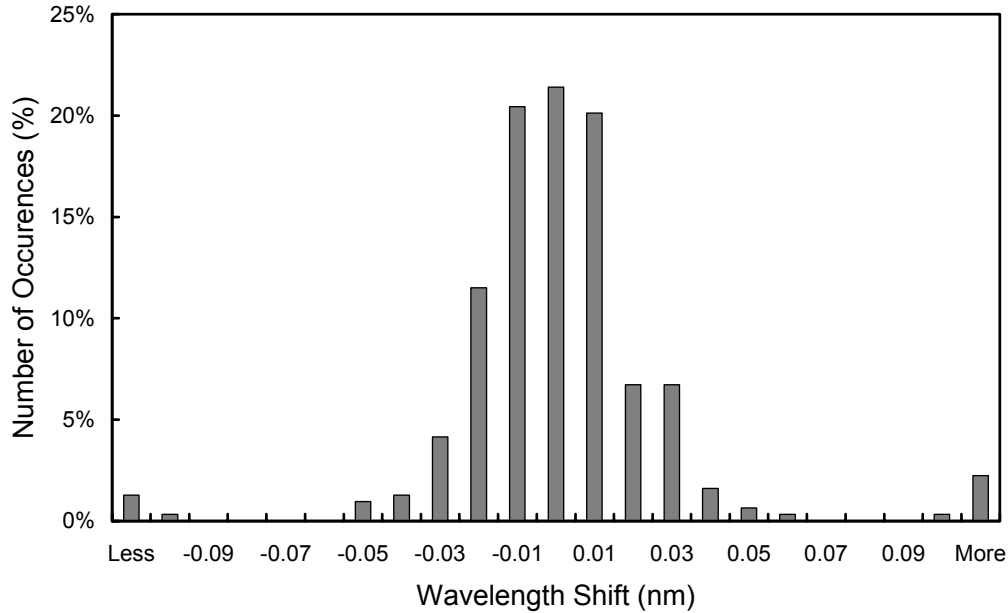


Figure 5.4.9. Differences in the measured position of the 296.73 nm mercury line between consecutive wavelength scans. The labels of the horizontal axis give the center wavelength shift for each column. The 0-nm histogram column covers the range from -0.005 to +0.005 nm. “Less” means shifts smaller than -0.105 nm; “more” means shifts larger than 0.105 nm.

The defective air-conditioner of the system also affected the temperature stability of the monochromator. Since it can be expected that these temperature fluctuations influence the wavelength stability of the monochromator, wavelength shifts were examined for every spectrum performed in a time period when temperature changes were largest. Figure 5.4.12 shows wavelength shifts calculated with the Fraunhofer method together with monochromator temperature for the period 11/25/99 – 12/10/99. This period includes the most extreme day of the season when the monochromator temperature rose to almost 42°C on 12/1/99. Figure 5.4.12 shows that this temperature increase is correlated with a 0.04 nm change in wavelength registration. This change is smaller than initially expected and compares well with typical day-to-day fluctuations in the wavelength setting. For example, between 12/3/99 and 12/8/99 the wavelength setting fluctuates by 0.05 nm and the temperatures are only slightly above the set-point of 33°C.

Although data from the external mercury scans do not have a direct influence on the data products, they are an important part of instrument characterization. Figure 5.4.13 illustrates the difference between internal and external mercury scans collected during both site visits. The wavelength scale of the figure is the same as applied during solar measurements. The peak of the external scans, agrees approximately with the nominal wavelength of 296.73 nm, whereas the peak of the internal scans is shifted about 0.16 nm to shorter wavelengths. External scans have a bandwidth of about 1.05 nm FWHM, whereas the bandwidth of the internal scan is only 0.70 nm. As external scans have the same light path as solar measurements, they more realistically represent the monochromator bandpass relevant to solar scans. Scans at the start and end of the season are consistent.

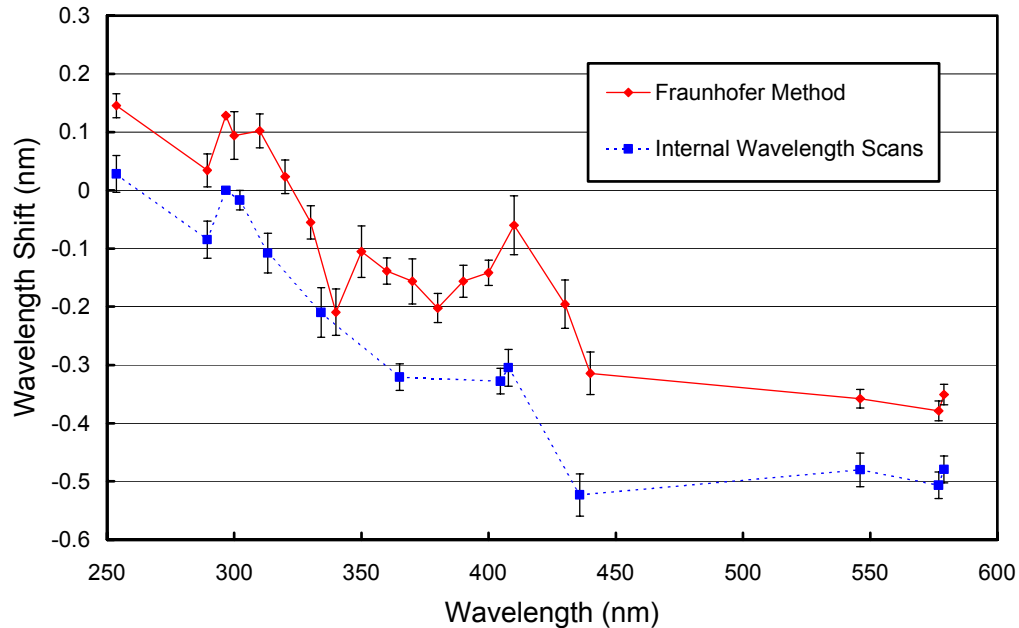


Figure 5.4.10. Monochromator non-linearity for the Ushuaia 1999-2000 season. Heavy line: Correction function calculated with the Fraunhofer-correlation method, applied to correct the Ushuaia Volume 9 data. Thin broken line: Correction function calculated with the method that was historically applied. The offset difference between both methods is 0.15 nm. The error bars are the 1σ standard deviation of the wavelength shift for the season.

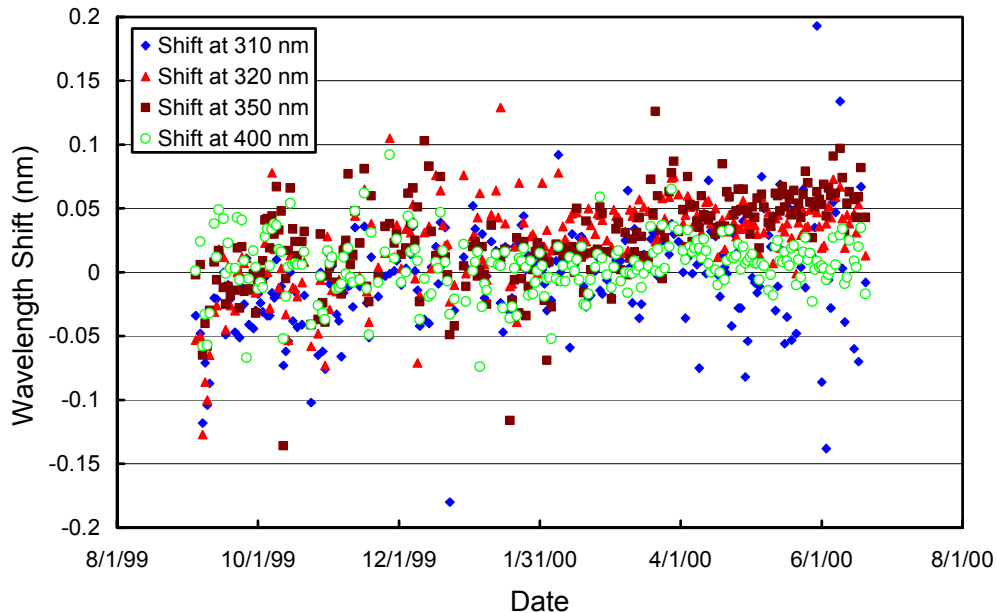


Figure 5.4.11. Wavelength accuracy check of the final Ushuaia Volume 9 data at four wavelengths by means of Fraunhofer correlation.

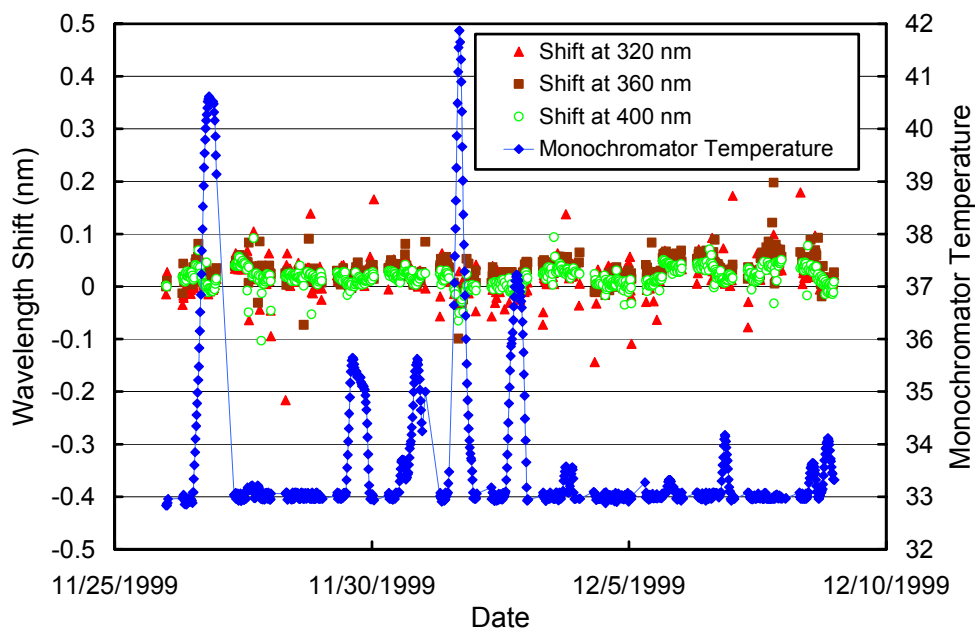


Figure 5.4.12. Wavelength shifts of final Ushuaia data in comparison with monochromator temperature for the period 11/26/99 – 12/08/99.

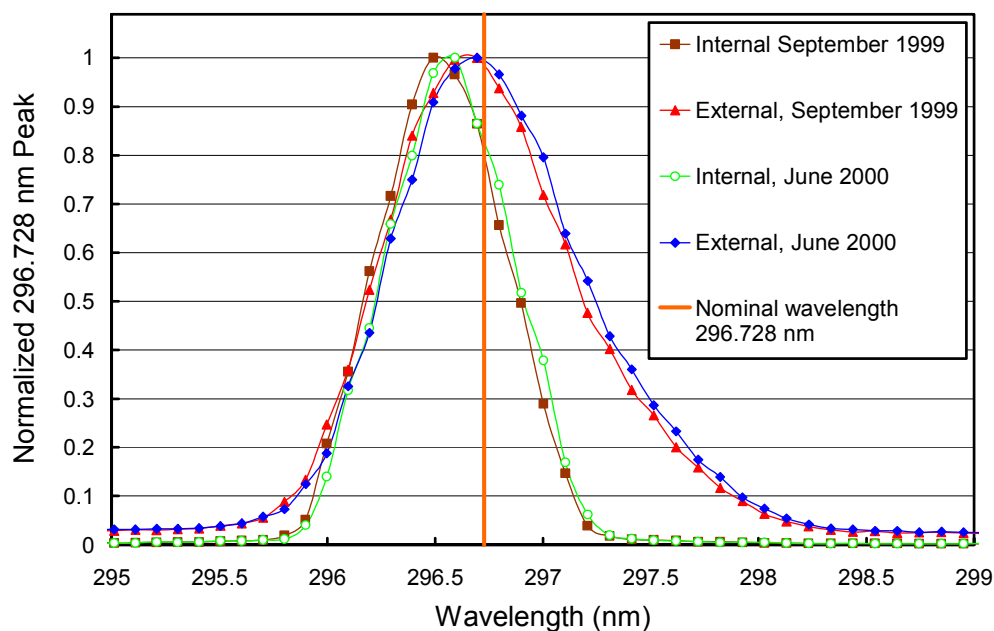


Figure 5.4.13. The 296.73 mercury line as registered by the PMT from external and internal sources. The wavelength scale is the same as applied for solar measurements, i.e., it is based on a combination of internal scans and the Fraunhofer-correlation method. It is assumed that the wavelength registration of the monochromator did not shift between internal and external scans, which were close in time.

5.4.4. Missing Data

A total of 15469 scans are part of the published Ushuaia Volume 9 dataset. These are 97% of the scans scheduled. Approximately 2.2% of all scans were missed due to technical problems. Of all missing scans, 144 were superseded by absolute, and 23 by wavelength scans. Because of computer problems, 30 scans were missed on 9/15/99 and 8 scans on 12/1/99. Because of the defective A/C unit monochromator temperature exceeded 40 °C on 12/25/99 – 12/27/99. In order to protect the monochromator, the system switched off automatically, causing a loss of 94 scans. Because of the failure of internal irradiance standard and lamp power supply a total of 111 scans were missed between 11/12/99 and 11/17/99. Until the power supply was repaired, several manually performed response scans were conducted with a spare power supply between 11/17/99 and 12/10/99, superseding 19 data scans. Because of a full disk drive, 8 scans were missed on 2/16/00. Finally, a total of 65 files measured on various days throughout the season were found to be of insufficient quality and were excluded from the published data set.